Automatic Exploration and Morphometry/Morphology Assessment of Medical Image Databases

Alexandre Guimond, Gérard Subsol, Jean Meunier, Jean-Philippe Thirion

Automatic Exploration and Morphometry/Morphology Assessment of Medical Image Databases

Alexandre Guimond[a,b], Gérard Subsol[b], Jean Meunier[a], and Jean-Philippe Thirion[b]

[a]Département d'Informatique et de Recherche Opérationnelle
Université de Montréal, Montréal, Québec H3C 3J7 Canada

[b]Institut National de Recherche en Informatique et Automatique
Sophia Antipolis 06902 France

ABSTRACT

The design of representative models of the human body is of great interest to medical doctors. Qualitative information about the characteristics of the brain is widely available, but due to the volume of information that needs to be analyzed and the complexity of its structure, rarely is there quantification according to a standard model. To address this problem, we propose in this paper an automatic method to retrieve corresponding structures from a database of medical images. This procedure being local and fast, will permit navigation through large databases in a practical amount of time. We present as examples of applications the building of an average volume of interest and preliminary results of classification according to morphology.

Keywords: image database, exploration, volume of interest (VOI), average patient, medical atlas, classification, registration, magnetic resonance imaging (MRI)

1. INTRODUCTION

Neurological disorders like schizophrenia or Alzheimer's disease have for long been the subject of serious studies. It is believed that such conditions could be coupled with abnormal configurations of different brain structures, but strong quantitative evidence has still to be reported. Although anatomical brain atlases[1–4] provide information to analyze and compare brain structures, their characteristics, such as precise shape and variance among healthy subjects, are not yet clearly defined. Moreover, paper representations are not sufficient to answer today's problems in this field[5,6]; such atlases are two dimensional, static and based on one or few studies. Computer guided diagnosis, multimedia medical teaching or surgical simulation robotics require more adaptable and complete sources of information.

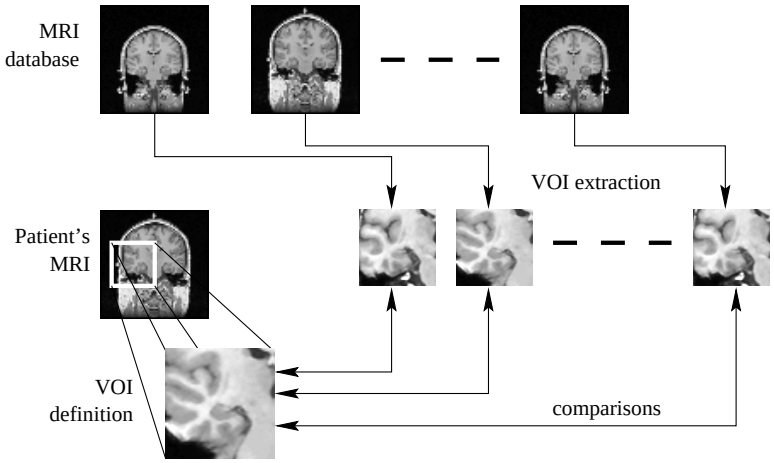

Figure 1. Volume of interest extraction and comparison are the principal ideas behind medical image database exploration.

Further author information –
A.G.(correspondence): Email: guimond@iro.umontreal.ca; WWW: http://www.iro.umontreal.ca/~guimond;
Telephone: (+514) 343-7107; Fax: (+514) 343-5834
G.S. Email: subsol@sophia.inria.fr; WWW: http://www.inria.fr/epidaure/personnel/subsol/subsol.html;
Telephone: (+33) (0)4 93.65.76.60; Fax: (+33) (0)4 93.65.76.69;
J.M.: Email: meunier@iro.umontreal.ca; WWW: http://www.iro.umontreal.ca/~meunier;
Telephone: (+514) 343-7107; Fax: (+514) 343-5834
J.P.T. Email: thirion@sophia.inria.fr; WWW: http://www.inria.fr/epidaure/personnel/thirion/thirion.html;
Telephone: (+33) (0)4 93.65.76.60; Fax: (+33) (0)4 93.65.76.69;

Over recent years, the use of magnetic resonance imaging (MRI) has produced huge medical brain image databases. Study of these data could provide the information needed to build numerical atlases with quantification of brain structure characteristics. This article addresses the problem of exploring such databases to retrieve information about a specific part of the brain (see Figure 1). The idea is to provide tools for practitioners to define a volume of interest (VOI) within a patient's MRI and extract corresponding VOIs from the database. These VOIs can be viewed as either control subjects or representative elements of different classes of pathology. In the first case, contrast images would facilitate the identification of significant abnormalities in the patient's VOI. In the second, comparisons would reveal which pathologies the patient is most related to, with associated probabilities. For example, to study temporal lobe epilepsy, we could use a database composed of representatives of a normal subject, of an epileptic with an atrophied left hippocampus and of an epileptic with an atrophied right hippocampus. Following the extraction of the hippocampus and comparisons, a diagnostic would be automatically produced putting forward affinities between the patient and the database elements.

The heart of such an extraction procedure is a matching method that finds correspondences between the patient's brain and the database elements. Once the VOIs extracted, we can apply different kinds of processing: automatic measure of features, shape extraction and comparison, factor analysis, statistical ordering, etc... Thus, we present a new method to evaluate differences between VOIs and obtain quantitative information from the database.

The first part of this paper reports different techniques used to compare brains. The second part deals with brain structure differences between individuals and the type of information they convey. We present our method in a third section, and explain how to identify important differences between images depending on the kind of information that we seek. The fourth part is an overview of possible applications including the construction of an average patient and some preliminary results of classification according to morphology. We conclude the paper with a brief discussion of future work.

2. MATCHING METHODS

Matching a model image I_m with a scene image I_s, using a transformation class T and a similarity measure S, can be formalized as the process of finding the function M that minimizes $S(M(I_m), I_s)$. The application of this function to the model image $M(I_m)$ will be called a *mapping*, or equivalently a *warping*, of I_m onto I_s.

2.1. Previous work

Many matching methods have been put forward to identify differences between brain images (see Ref. 7 for a comprehensive review). They can be divided in two main categories: feature based[8–11] and intensity based,[12–15] the trade-off being between the size of data to register and the complexity of the registration procedure.

The class of transformation T used is also of importance. Various approaches exist. To name a few, registration methods have been developed using linear,[16–18] piecewise linear,[19] quadratic[20] and free-form[12,13] classes (see Figure 2 for a rough classification).

A very common approach is to use the Talairach reference space, also known as the three-dimensional proportional grid system.[1] This system uses the intercommissural line and some other anatomical landmarks to partition the brain into twelve subspaces and is an attempt to model non-linear differences between data sets.

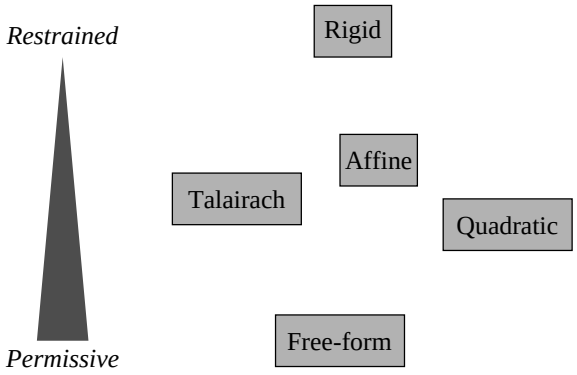

Figure 2. Classification of different transformation classes.

We can generalize the idea of Talairach by finding more landmarks, which leads to additional subdivisions of the brain volume and make the transformations more local. The difficulty lies in the automatic detection of the landmarks. A promising solution relying on differential geometry criteria can be found in Ref. 21.

2.2. Our matching method

The matching method we developed differs from previous work by confining itself to a VOI. This has several advantages. It corresponds to doctors' need of studying particular brain structures. It also reflects the assumption that gross anatomical shape is only influenced by neighboring bodies. Finally, the database investigation must be fast. Using sub-images will help us achieve this end.

We propose a new method to quantify differences between subjects in a localized volume of the brain using a three step approach that progressively refines the matching:

1. A global matching between the entire data sets.
2. A regional matching between corresponding VOIs.
3. A local matching in a voxel's neighborhood.

The matching procedure we use works as follows: given two images and a transformation class T, the algorithm delivers a mapping function M to warp a model image I_m onto a scene image I_s. In order to be less sensitive to the intensity values, a global bias and gain between the intensities of the two images can also be estimated by the algorithm. This gives us results qualitatively similar to Refs. 22,23 but with an implementation one or two orders of magnitude faster. More details can be found in Refs. 12,24.

3. BRAIN STRUCTURE VARIATIONS

3.1. Types

Variations between corresponding structures of different subjects can be separated in two categories:

Morphological These are differences due to the *presence* or the *absence* of a certain feature. For example, Figure 3 shows two different patients with morphological variations. The subject on the left has two gyri and the one on the right only one. These are non-trivial differences since they require to deduce the location of absent features.

Morphometrical These are variations due to the different properties of *existing* features. For example, the length of a gyri or the volume of the ventricles (Figure 3 presents two patients with different ventricle volumes). For the purpose of this article, morphometrical variations will be divided in three categories:

Global Brain scale morphometrical variations.

Regional VOI scale morphometrical variations.

Local Voxel scale morphometrical variations.

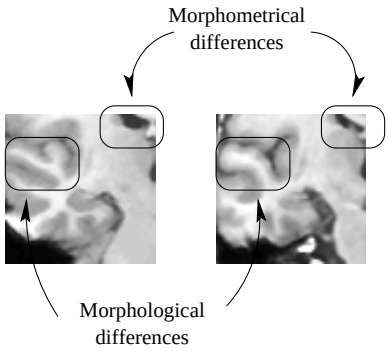

Figure 3. Morphometrical and morphological differences.

3.2. Irrelevant variations

As previously mentioned, our interest lies in the study of particular brain structures. In that respect, it is generally agreed that for the vast majority of subjects, global morphometrical differences, such as whole brain width or length, are not really significant. Furthermore, this idea can hold for differences between sufficiently large VOIs. Our registration method will reflect those assumptions by correcting for affine differences at global and regional scales. This class of transformation will correct translation, rotation, scale and skew differences between VOIs.

Choosing this transformation class has some advantages over the Talairach alternative. The proportional grid system is a reference space that is frequently used by medical doctors, which is an important asset since they are the end-users. But it shows poor accuracy when matching structures away from the anterior and posterior commissures and limits the extraction procedure to the brain.

It is worth noting that correcting for affine differences between VOIs is in agreement with Talairach's philosophy of not considering structures away from the ones of concern. Since they are both based on linear transformations, their differences can be estimated by looking at the number of free parameters they hold. A Talairach conversion is defined by 1 3D point, 1 distance (from AC to PC), 1 rotation around each axis and 6 scaling factors for a total of 13 unknowns. An affine transformation accounts for 12 parameters: 1 3D translation and for each axis, 1 rotation, 1 skew and 1 scaling. So there is only 1 degree of freedom difference between them.

4. EXTRACTION OF VOI

4.1. Method

As mentioned earlier, our method is divided into three steps: (1) global, (2) regional and (3) local matching to evaluate global, regional and local morphometrical differences respectively. These steps are detailed below and displayed in Figure 4.

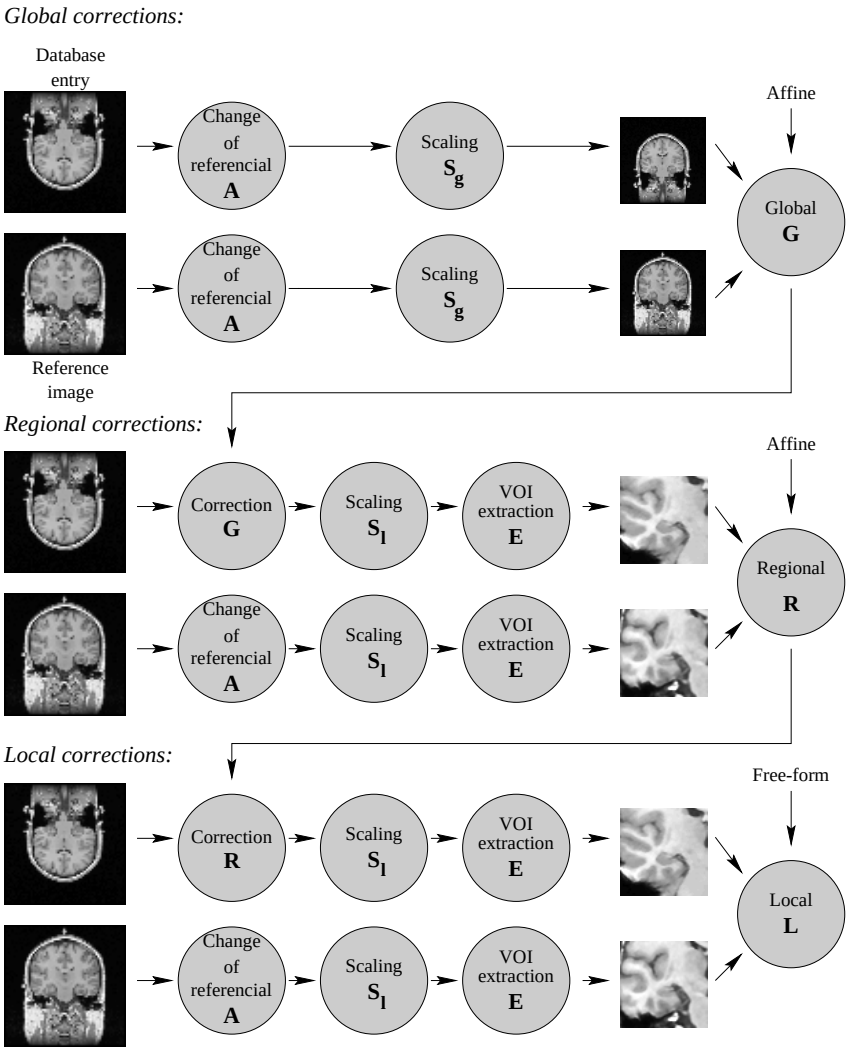

Figure 4. VOI extraction method using the reference image and a database entry.

Global morphometrical corrections
The global correction procedure consists in *estimating* an affine transformation to map the database entry's dimensions to the ones of the reference image. This step is necessary to extract roughly corresponding VOIs needed for regional comparisons in the second step. To reduce computation, the matching is done on sub-sampled images, a justifiable approach since we are only looking for a rough correspondence.

Before registration, we apply to each of the two images the following transformations:

1. A transformation A to a standard axis view and voxel size. In our case these are coronal views and $1 \times 1 \times 1$ mm^3 per voxel. This transformation assures images coming from different sources are comparable.
2. A resampling using the scale parameter S_g to the desired resolution for global registration. In practice, this is a useful parameter that influences the precision of the transformation obtained and the computation time.

After matching, we obtain the global affine transformation G.

Regional morphometrical corrections This procedure is similar to the previous one. Two steps differ. The first modification concerns the database entry for which we substitute the change of referential by the global

correction matrix G. As a second difference, the scaling factor for global registration S_g is replaced by it's local equivalent S_l and a transformation E accounting for the VOI extraction. This last transformation is a cropping at identical locations for both images. In our work, it is implemented using a translation, to make it representable using matrices, and a size specification. This matching provides the regional affine transformation R.

Local morphometrical corrections Evaluation of local differences is done using the same procedure as before, with a correction matrix R updated with regional information, and a matching allowing a transformation class T of the free-form type.

Images after the regional correction are called *corresponding volumes of interest*. They differ only by morphological and local morphometrical variations. Hence, when considering structures of the same morphology, those images can be used to obtain information concerning morphometrical dissimilarities such as size differences.

Morphological variations can be obtained by applying the third step that corrects for local morphometrical differences. From this, the detection of particular features could be obtained.

An interesting aspect of our work is the combination of those transformations by way of 4×4 matrices in homogeneous coordinates, and optionally a displacement field derived from local variations, to end up with a single transformation and therefore a single resampling of the raw images.

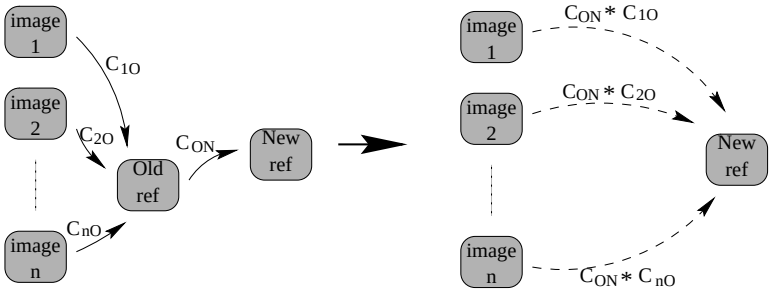

Figure 5. Matrix combination to change the reference image.

It is also possible to completely eliminate the first part of the procedure since, for a given reference image, these transformations do not depend on the VOI definition. They can be precomputed to save time. Moreover, when the reference image changes, instead of recomputing the whole set of global transformations, it is sufficient to combine them with the transformation that brings the old reference image onto the new one (see Figure 5).

4.2. Data sets

The following results were obtained using a database of 10 MR images of healthy subjects provided by Dr. Ron Kikinis of Brigham and Women's Hospital (see Figure 6). Each image contains $256\times256\times123$ voxels each representing $1 \times 1 \times 1.5$ mm^3 with a possibility of 256 gray levels. A coronal slice of each of those images is shown in Figure 6 in which the subject's left side corresponds to the left side of the image . The images will be called $I_1, \ldots, I_{10}$, referring to the corresponding image when counting from left to right, top to bottom. All experiments were conducted on a DEC AlphaStation 400 4/233.

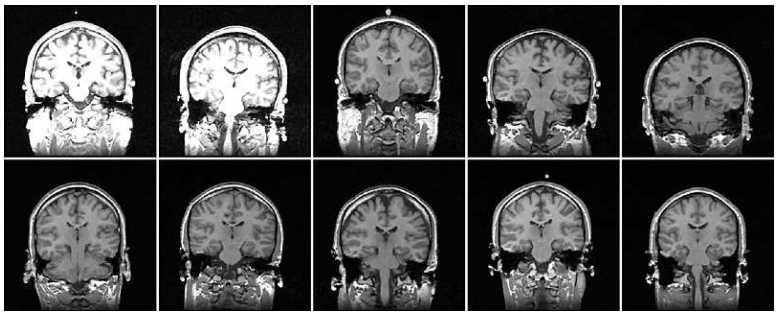

Figure 6. Coronal slice of each image composing the database. Images are numbered from 1 to 10 when counting from left to right, top to bottom.

4.3. Results

We present the correction of morphometrical differences for a VOI in the left temporal lobe of the brain. The reference image is I_{10} in which we define a VOI of $64 \times 64 \times 20$ voxels of $1 \times 1 \times 1$ mm^3.

Figure 7 shows the evolution of the VOIs throughout the correction procedure. The first image, Figure 7(a), presents the VOIs taken before any processing. It exhibits the differences due to intensity and positioning. After the first step which consists of intensity corrections and elimination of global morphometrical differences, the VOIs seem much more similar (see Figure 7(b)).

Although affine dissimilarities are small, it is still possible to eliminate those variations by matching only the VOI images instead of the whole brain volume. Results of this second phase are shown in Figure 7(c). They represent corresponding VOIs and their differences are due only to morphology and local morphometry.

The third step is to eliminate those local morphometrical differences. After this (see Figure 7(d)), we believe that only morphological differences are present.

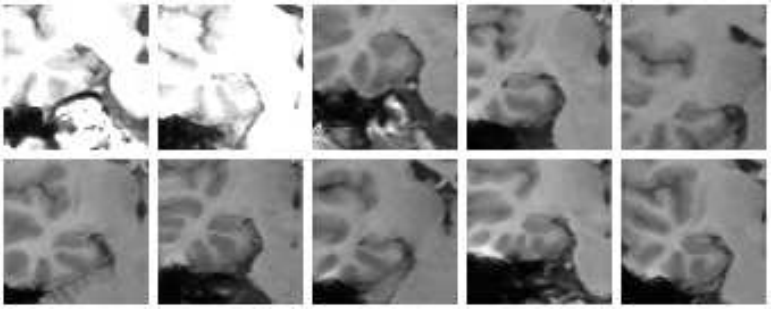

(a) VOIs without correction.

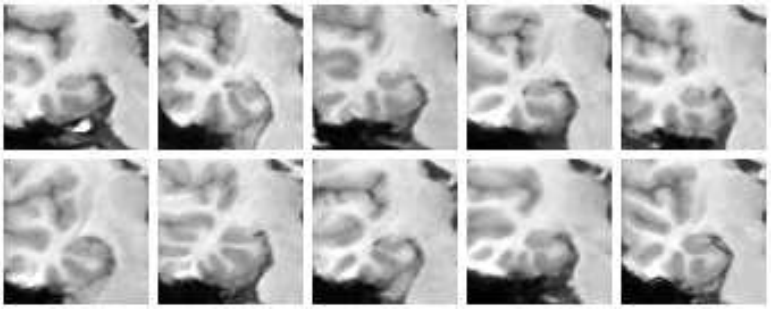

(b) VOIs after global correction.

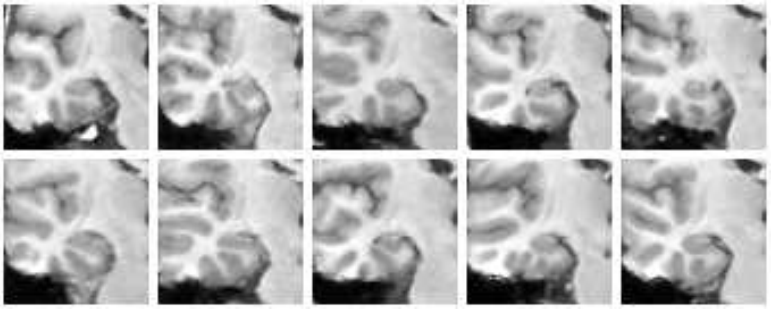

(c) VOIs after regional correction.

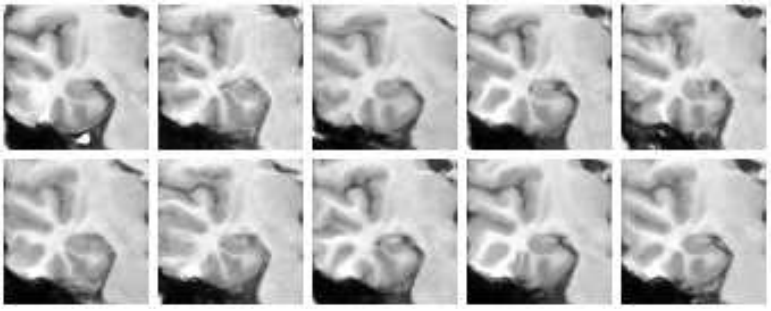

(d) VOIs after all morphometrical corrections.

Figure 7. VOI Extraction

5. APPLICATIONS

Applications resulting from the correction of morphometrical differences could be divided in two categories: (1) studies of local morphometrical differences or (2) studies of morphological variations.

5.1. Morphometrical measures

This class of application relies on measures of brain structures. For example, the comparisons of the basal ganglia's components volumes with a standard model to identify schizophrenia.[25] The construction of such a model relies on measures taken from a population of normal subjects. We have implemented this last idea.

5.1.1. Construction method

The idea behind the construction procedure is derived from Refs. 8,26,27,16 and consists of extracting from the database the volumes corresponding to a VOI defined on a reference image, and applying to the average of those VOIs the average of the local morphometrical differences. This process is depicted in Figure 8.

Using the procedure described in section 4.1. on all the entries of the database, we can eliminate global and regional morphometrical differences to extract corresponding VOIs of our database. For each of those entries, we can compute the displacement field that maps the entry VOI onto the reference VOI (forward) and the reference VOI onto the entry VOI (backward). These displacements account for local morphometrical differences. Applying to every region the forward displacement

field produces images with the same morphometry as the reference VOI but with different intensities. Arithmetic averaging of corresponding voxel's intensities between VOIs produces a mean intensity image with the morphometry of the reference image. Furthermore, by applying the average backward displacement field to this last image, we create a mean intensity and morphometry representation of our database, or the "average" VOI.

5.1.2. Resulting "average" patients

Figure 9 shows different kinds of "average" VOIs of the right temporal lobe. The first image is the reference VOI and is shown only for comparison purposes. To its right is a simple average of the VOIs taken from each subject previous to any warping, putting forward the different patient positions during the acquisition. The third image presents the average of corresponding volumes of the database. Structures which are morphologically stable appear well contrasted while unstable ones are fuzzy. The first image of the second line is the average of the VOI intensities after elimination of morphometrical differences. Deforming this image with the average backward displacement field creates an image that represents the mean intensity and morphometry of the database, or the average VOI. It has the remarkable property of being an average image while not suffering from severe smoothing. Finally, we present the variance of the backward deformation fields' amplitude obtained from our database as a simple display of the variability of the different structures positions.

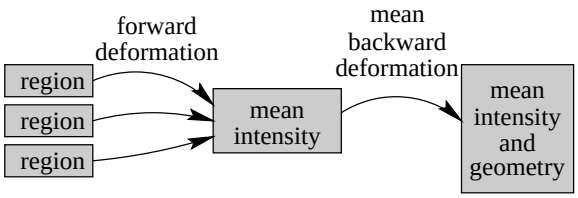

Figure 8. Procedure to build an average VOI from a set of images.

An advantage of our technique is that the average images it produces are of quality similar to the MR images of the database. Hence the same inter-patient matching method can be applied to compare a new patient to the average, which is an alternative to whole database exploration.

We have applied the same scheme to extract from the database the volumes that contain the ventricles. Averages have been built using the method previously explained and are shown in Figure 10(a). The careful observer will notice that, although they were obtained using different methods, the average VOI (last image of the second row) resembles a smoothed version of the average VOI after affine correction (last image of the first row). This is especially true for the ventricles and strengthens the theory behind our method.

In this case, we have also applied to the segmented ventricles, the displacement field corresponding to the average local morphometrical differences. This permitted to construct ventricles that represent the average morphometry of our database. They are shown in Figure 10(b). To the left, the original ventricles and to it's right, a display of their average morphometry. An obvious difference is the back-end of the ventricles which are thinner for the average patient than for the original ventricles.

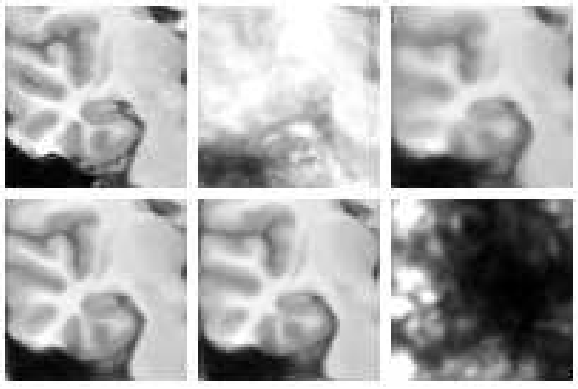

Figure 9. Different types of "average" patients. **First line**: Original reference VOI; average of the 10 VOIs before any processing; average VOI after exclusion of global and regional morphometrical differences. **Second line**: average VOI without morphometrical differences (mean intensity); average backward deformation applied to the average VOI without morphometrical differences (mean intensity and morphometry); variance of the average backward deformation. See the text for explications.

5.2. Morphological measures

This class of applications is concerned with the presence or absence of features. Following this, we have just begun experiments to classify similar patients according to their morphology. This work requires methods related to sorting subjects, or more generally, the development of similarity criteria. Their is a large literature on this topic[28,29] but our goal here is neither to find the best measure nor to analyze its relationship with our registration procedure. We wish to show practical applications of VOI extraction and evaluate qualitatively different similarity criteria. Hence, the following experiments are to be considered as a

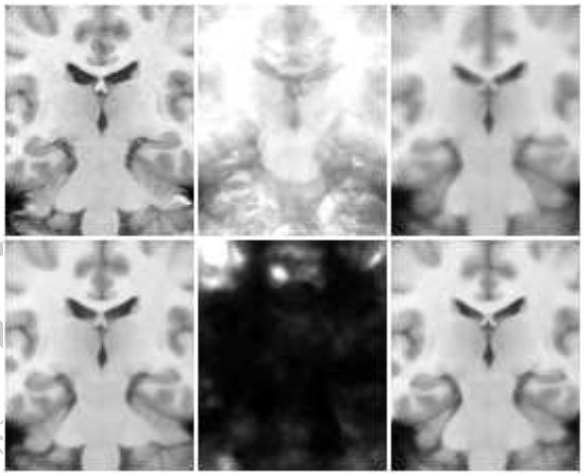

(a) Average VOI obtained from free-form registration (see Figure 9 for explanations. The positions of the second and third images of the second line have been interchanged for comparison purposes.).

(b) **Left**: original ventricles. **Right**: morphometrical average ventricles of the database.

Figure 10.

first step of a feasibility study. Furthermore, the images at our disposal are of normal subjects. Consequently, we are not trying to evaluate pathologies or find anomalies.

Among available choices, we have chosen two: (1) the stochastic sign-change (SSC), which is based on zero-crossings, and (2) correlation. The method consists of extracting morphometrically corresponding VOIs automatically from the database using the method previously described. We then define a *working space* in which comparisons are done (see Figure 11). We present the criteria used and show preliminary results of VOI classification according to their resemblance with I_{10}.

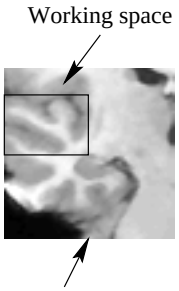

Figure 11. A slice of the VOI and working space. Only the working space is considered for comparisons.

5.2.1. The stochastic sign-change criterion

This criterion was introduced by Venot *et al.*[30] for the comparison of scintigraphic images. It is a measure of similitude between two images and is based on zero-crossings (see Figure 12).

Let I_1 and I_2 be similar images that contain noise and $S = I_1 - I_2$. Originally, I_1 and I_2 are identical. Then, S is not zero but contains sign fluctuations because of noise. However, if the two images differ from one another in some region R of S, R will contain either mostly positive or mostly negative values and the number of sign changes in S is reduced. This shows that a high SSC count in S is a good indication of resemblance between two images.

To count the number of sign changes, we go through the subtraction image three times. Once comparing values in the X direction, once in the Y direction and a last time for the Z direction. This criterion can be normalized by considering the maximal value of SSC in the working space. Hence, values close to 1 shows good similitudes, and those close to 0, poor correspondence.

5.2.2. Correlation

The correlation between two working spaces X and Y each containing N voxels is computed using the following formula:

$$\mathbf{Corr}(X,Y) = \frac{\mathbf{Cov}(X,Y)}{\sqrt{\mathbf{Var}(X)\mathbf{Var}(Y)}}$$

where

$$\begin{aligned} \mathbf{Cov}(X,Y) &= \frac{1}{N}\sum_{i=1}^{N} X_i Y_i - \frac{1}{N^2}\sum_{i=1}^{N} X_i \sum_{i=1}^{N} Y_i \\ \mathbf{Var}(X) &= \mathbf{Cov}(X,X) \\ \mathbf{Var}(Y) &= \mathbf{Cov}(Y,Y) \end{aligned}$$

5.2.3. Results

The SSC values and correlation coefficients are shown sorted in Table 1. We also present, using this ordering, the working spaces used for computations in Figures 13(a) and 13(b). Each of these figures contains two non-adjacent slices of the VOIs to get a better understanding of the tridimensional structure. They show the importance of our three dimensional approach since one would probably change this ordering by only looking at one slice.

The ordering obtained with the SSC criterion and with correlation are similar up to minor permutations. The only large difference has to do with I_1 which is identified as having the most different morphology using the SSC criterion and is place fifth using correlation. By looking at both slices of this VOI, we can see that it is quite similar to I_{10}. Hence, preliminary results seem to indicate that correlation would be more appropriate to evaluate morphological differences than the SSC criterion. In light of those results, comparisons based on mutual information techniques are expected to give good classifications.

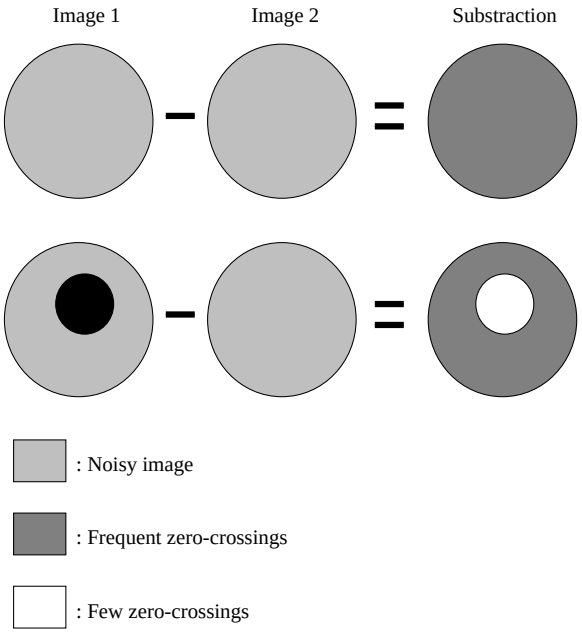

Figure 12. The stochastic sign-change criterion.

Although in this case we used an elastic registration procedure before classification, when assuming negligible morphological variations, this classification method can be used on corresponding VOIs thus using only affine transformation for registration purposes. In this case, an order on local morphometrical differences would be obtained.

Image	SSC value (normalized)
10	1.000
4	0.325
7	0.315
6	0.305
9	0.285
5	0.284
3	0.282
2	0.279
8	0.271
1	0.268

Image	Correlation
10	1.000
4	0.917
6	0.906
3	0.906
1	0.888
7	0.879
5	0.858
9	0.845
8	0.844
2	0.836

Table 1. Classification using the SSC criterion (left) and correlation (right).

5.3. Discussion

The main benefit of this method is that it is fast and fairly robust. The time to obtain the corresponding VOIs varies between 5 and 10 seconds, and local warping doubles this time. This opens a new door on medical image database exploration. It is now possible to retrieve a large amount of corresponding volumes in a reasonable amount of time. Once those volumes extracted, further processing like classification and similarity matches can be operated to result into extrapolation of information contained in the database to other images. For example, this technology is presently being used for the study morphometrical hippocampal variations in epileptic patients. We have only started to explore this field but preliminary results are encouraging.

6. CONCLUSION

We have presented a new method to obtain corresponding volumes of interest from medical image databases. This procedure has the advantage of restraining itself to local volumes of the brain and thus is not influenced by misleading information from other regions. It has been applied to the quantification of morphometrical and morphological variations. We believe that better results could be obtained by dividing subjects into subclasses of normal patients based on morphological similarities. This would facilitate the analysis of only morphometrical differences, to provide a better understanding of dissimilarities between a patient and the group of normal subjects with corresponding morphology.

Future applications and research on classification and extraction of similar patients for epidemiology statistics or computer aided diagnosis are envisioned. Such applications are a first step toward the extrapolation of information from an image database to other images.

ACKNOWLEDGEMENTS

Thanks to Dr. Ron Kikinis of Brigham and Women's Hospital, Boston, for the MR images. Part of this work was funded by the Natural Sciences and Engineering and Research Council of Canada (NSERC), the Fonds pour la Formation de Chercheurs et l'Aide à la Recherche du Quàbec (FCAR), the Association des Directeurs de Recherche Industrielle du Quàbec (ADRIQ) and the Dàpartement d'Informatique et de Recherche Opàrationnelle de l'Universitàde Montràal (DIRO).

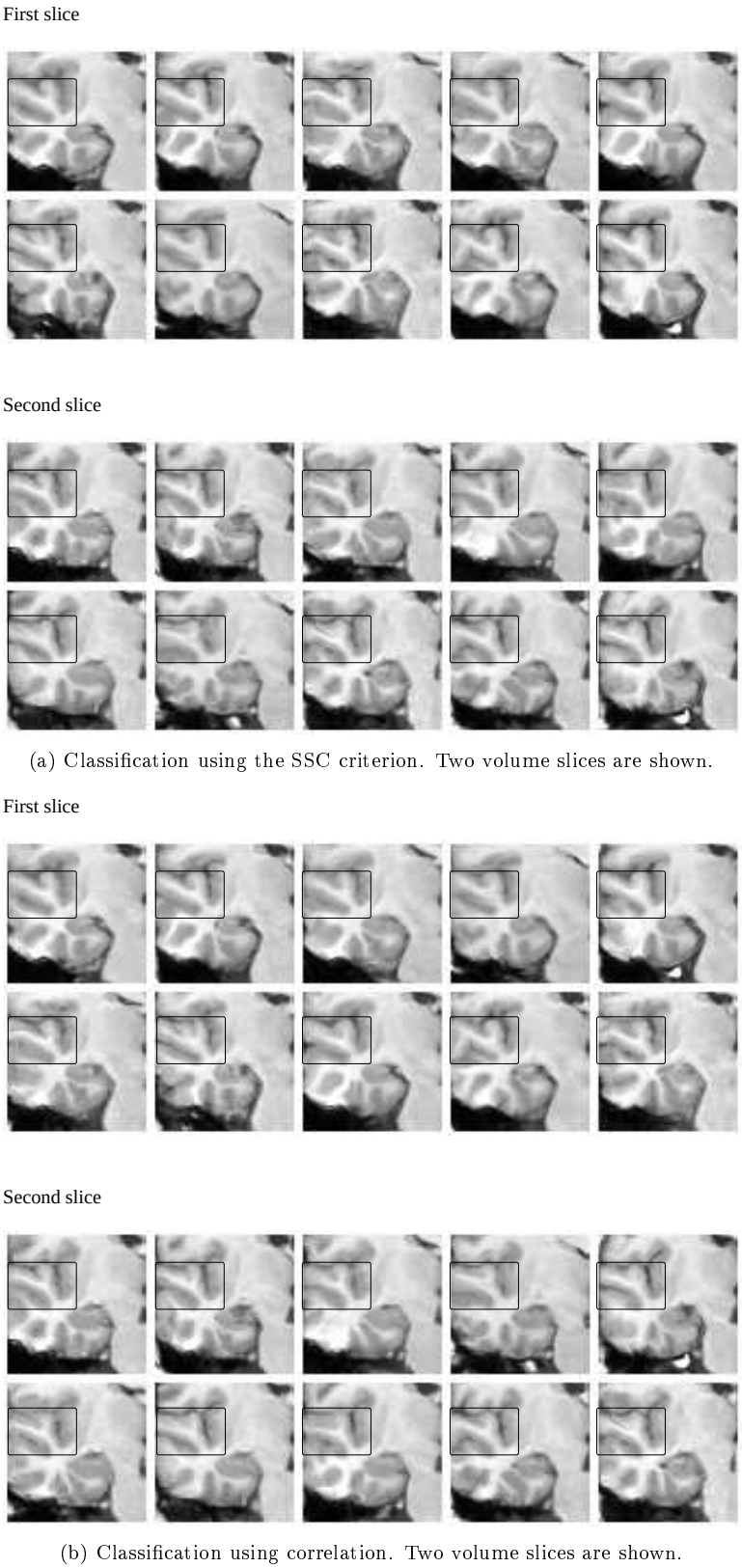

(a) Classification using the SSC criterion. Two volume slices are shown.

(b) Classification using correlation. Two volume slices are shown.

Figure 13. Classifications.

REFERENCES

1. J. Talairach and P. Tournoux, *Co-Planar Stereotaxic Atlas of the Human Brain*, Thieme Medical Publishers, New York, United-States, 1988.
2. G. Schaltenbrand and W. Wahren, *Atlas of Stereotaxy of the Human Brain*, Georg Thieme Verlag, Stuttgart, 1977.
3. E. Pernkopf, *Atlas d'anatomie humaine*, Piccin, 1983.
4. H. Braak, *Architectonics of the human telencephalic cortex*, Springer-Verlag, Berlin, 1980.
5. J. C. Mazziotta, A. W. Toga, A. Evans, P. Fox, and J. Landcaster, "A probabilistic atlas of the human brain: Theory and rationales for its development," *Neuroimage* **2**, pp. 89–101, 1995.
6. G. Subsol, *Construction automatique d'atlas anatomiques morphométriques é partir d'images médicales tridimensionnelles*. PhD thesis, à cole Centrale de Paris, 1995.
7. A.W. Toga, P. Thompson, and B. A. Payne, *Modeling Morphometric Changes of the Brain During Development*, Academic Press, 1996.
8. G. Subsol, J.-P. Thirion, and N. Ayache, "Application of an automatically built 3D morphometric brain atlas: Study of cerebral ventricle shape," in *Visualisation in Biomedical Computing*, K. H. Hàhne and R. Kikinis, eds., vol. 1131 of *Lecture Notes in Computer Science*, pp. 373–382, Springer Verlag, (Hamburg (Germany)), Sept. 1996.
9. A. Guàziec and N. Ayache, "Smoothing and matching of 3D space curves," in *Europeen Conference on Computer Vision*, Springer-Verlag, (Santa Margherita (Italy)), May 1992.
10. J. Feldmar and N. Ayache, "Rigid, Affine and Locally Affine Registration of Free-Form Surfaces," *International Journal of Computer Vision* **18**, pp. 99–119, May 1996. Electronic version: http://www.inria.fr/RRRT/RR-2220.html.
11. R. Szeliski and S. Lavallàe, "Matching 3-D Anatomical Surfaces with Non-Rigid Deformations using Octree-Splines," *International Journal of Computer Vision* **18**, pp. 171–186, May 1996.
12. J.-P. Thirion, "Fast non-rigid matching of 3D medical images," in *Medical Robotics and Computer Aided Surgery*, pp. 47–54, (Baltimore (USA)), Nov. 1995. Electronic version: http://www.inria.fr/RRRT/RR-2547.html.
13. D. L. Collins, T. M. Peters, and A. C. Evans, "An automated 3D non-linear deformation procedure for determination of gross morphometric variability in human brain," in *Visualisation in Biomedical Computing*, R. A. Robb, ed., vol. 2359 of *SPIE Proceedings*, pp. 180–190, (Rochester), Oct. 1994.
14. J. Gee, M. Reivich, and R. Bajcsy, "Elastically deforming 3D atlas to match anatomical brain images," *Journal of Computer Assisted Tomography* **17**(2), pp. 225–236, 1993.
15. M. Bro-Nielsen and C. Gramkow, "Fast Fluid Registration of Medical Images," in *Visualization in Biomedical Computing*, K. H. Hàhne and R. Kikinis, eds., vol. 1131 of *Lecture Notes in Computer Science*, pp. 267–276, Springer, (Hamburg (Germany)), Sept. 1996.
16. D. L. Collins, P. Neelin, T. M. Peters, and A. C. Evans, "Antomatic 3D intersubject registration of MR volumetric data in standardized Talairach space," *Journal of Computer Assisted Tomography* **18**, pp. 1992–205, Mar./Apr. 1994.
17. N. C. Andreasen, S. Arndt, V. Swayze II, T. Cizadlo, M. Flaum, D. O'Leary, J. C. Ehrhardt, and W. T. Yuh, "Thalamic abnormalies in schizophrenia visualized through magnetic resonance image averaging," *Science* **266**, pp. 294–298, 1994.
18. J. Martin, A. Pentland, S. Sclaroff, and R. Kikinis, "Characterization of neuropathological shape deformations," Tech. Rep. 331, M.I.T. Media Laboratory Perceptual Computing, May 1995.
19. D. Lemoine, C. Barillot, B. Gibaud, and E. Pasqualini, "An anatomical-based 3D registration of multimodality and atlas data in surgery," in *Information Processing in Medical Imaging*, A. Colchester and D. Hawkes, eds., p. 188, Springer-Verlag, (Wye (UK)), 1991.
20. T. Greitz, C. Bohm, S. Holte, and L. Eriksson, "A computerized brain atlas: Construction, anatomical content, and some applications," *Journal of Computer Assisted Tomography* **15**, pp. 26–38, Jan. 1991.
21. J. Declerck, G. Subsol, J.-P. Thirion, and N. Ayache, "Automatic retrieval of anatomical structures in 3D medical images," in *Conference on Computer Vision, Virtual Reality and Robotics in Medecine*, N. Ayache, ed., vol. 905 of *Lecture Notes in Computer Science*, pp. 153–162, Springer-Verlag, (Nice (France)), Apr. 1995. Electronic version: http://www.inria.fr/RRRT/RR-2485.html.

22. R. Bajcsy and S. Kovaàià, "Multiresolution elastic matching," *Computer Vision, Graphics and Image Processing* **46**, pp. 1–21, 1989.
23. G. E. Christensen, M. I. Miller, and M. Vannier, "A 3D brain mapping using a deformable neuroanatomy," *Physics in Medecine and Biology* **39**, pp. 609–618, 1994.
24. J.-P. Thirion, "Non-rigid matching using demons," in *Computer Vision and Pattern Recognition*, (San Francisco (USA)), June 1996. Electronic version: http://www.inria.fr/RRRT/RR-2547.html.
25. H. Hokama, M. E. Shenton, P. G. Nestor, R. Kikinis, J. J. Levitt, D. Metcalf, C. G. Wible, B. F. O'Donnell, F. A. Jolesz, and R. W. McCarley, "Caudate, putamen, and globus pallidus volume in schizophrenia: A quantitative MRI study," *Psychiatry Research: Neuroimaging* **61**, pp. 209–229, 1995.
26. G. Subsol, J.-P. Thirion, and N. Ayache, "A general scheme for automatically building 3D morphometric anatomical atlases: applications to a skull atlas," in *Medical Robotics and Computer Aided Surgery*, pp. 226–233, (Baltimore (USA)), Nov. 1995. Electronic version: http://www.inria.fr/RRRT/RR-2586.html.
27. J.-P. Thirion, G. Subsol, and D. Dean, "Cross validation of three inter-parients matching methods," in *Visualisation in Biomedical Computing*, K. H. Hàhne and R. Kikinis, eds., vol. 1131 of *Lecture Notes in Computer Science*, pp. 327–336, Springer-Verlag, (Hamburg (Germany)), Sept. 1996.
28. K. Fukunaga, *Introduction to Statistical Pattern Recognition*, Computer science and scientific computing, Academic Press, second ed., 1990.
29. T. Pavlidis, *Structural Pattern Recognition*, vol. 1 of *Springer series in electrophysics*, Springer-Verlag, New-York, 1977.
30. A. Venot, J. Lebruchec, J. Golmard, and J. Roucavrol, "An automated method for the normalization of scintigraphic images," *Journal of Nuclear Medicine* **24**, pp. 529–531, 1983.